ELSEVIER

Chemical Engineering Journal 137 (2008) 443–452

Chemical Engineering Journal

www.elsevier.com/locate/cej

One-step synthesis of chromium and aluminium containing SBA-15 materials
New phillips catalysts for ethylene polymerization

J. Aguado, G. Calleja, A. Carrero *, J. Moreno

Department of Chemical and Environmental Technology, ESCET, Rey Juan Carlos University, 28933 Móstoles, Madrid, Spain

Received 31 March 2007; received in revised form 25 June 2007; accepted 27 June 2007

Abstract

New CrAlSBA-15 mesoporous materials have been prepared by direct synthesis and characterized by ICP-AES, XRD, N_2 adsorption, ^{27}Al NMR, TEM, UV–vis and H_2-TPR. CrAlSBA-15 materials exhibited high mesostructural order starting from chromium(III) nitrate (Si/Cr = 66; Si/Al = 35 at pH 3) and from chromium(III) acetate hydroxide (Si/Cr = 39; Si/Al = 51 at pH 1.5). The incorporation of chromium and aluminium into SBA-15 mesoporous structure is enhanced by increasing the pH and produces an increase in pore size and pore volume. After calcination, samples prepared by one-step synthesis showed Cr(VI) centres well dispersed with a proportion of chromate species higher than Cr/AlSBA-15 catalysts prepared by impregnation and grafting. H_2-TPR measurements showed that only the 80% of Cr(VI) ions incorporated into the SBA-15 structure were reduced, so part of chromium ions may be located in non-accessible positions inside the solid walls.

CrAlSBA-15 materials obtained by direct synthesis exhibited higher ethylene polymerization activity (381.1 kg PE/g Cr h) than Cr/AlSBA-15 and conventional Cr/SiO_2 Phillips catalyst prepared by impregnation (260.5 and 216 kg PE/g Cr h, respectively).

Keywords: SBA-15; Direct synthesis; Chromium; Ethylene polymerization; Phillips catalysts

1. Introduction

The Phillips catalysts (chromium supported on amorphous solids like silica and silica-alumina) are presently used to produce more than one third of all polyethylene sold worldwide, being therefore its improvement a matter of great importance for many researchers [1–3]. Recently published works have been focused on the use of mesostructured silicas and silica-aluminas (MCM-41, Al-MCM-41, SBA-15 and Al-SBA-15) to prepare novel Phillips catalysts with very promising behaviours [4–8]. These investigations show that mesostructured materials allow preparing Phillips catalysts with very high activities in ethylene polymerization. These studies have also proved that the activity in the ethylene polymerization reactions is higher when using SBA-15 mesoporous silica than when using MCM-41 mesoporous silica [5–7]. Specifically, Phillips catalysts based on aluminium-containing SBA-15 materials are much more active than Cr/SBA-15 catalysts [8]. The incorporation of chromium centres in these new catalytic systems was carried out by post-synthesis methods (impregnation or grafting) and, then, a high temperature calcination (500–600 °C) step followed to produce Cr(VI) active species. Thus, two calcination process are necessary to prepare chromium polymerization catalysts using mesostructured materials, the first one to remove the surfactant molecules and obtain a porous support and the second one to get chromium(VI) centres anchored onto the support surface. It is obvious that the addition of chromium species directly into the synthesis gel of mesostructured materials would allow to prepare new Phillips catalyst by a more simple procedure since post-synthesis treatments and additional calcination steps would not be necessary.

The incorporation of transition metals into the framework of mesostructured SBA-15 material by direct synthesis has become a very attractive subject for many researchers because the heteroatom incorporation into the silica structure is carried out in only one step and more stable and dispersed metal species are obtained [9]. So, Yue et al. reported a successful direct method to prepare aluminium-containing SBA-15 with Si/Al ratios equal to 10 and 20 by a hydrothermal procedure at pH 1.5 using aluminium tri-*tert*-butoxide as a precursor [10]; Melero

* Corresponding author. Tel.: +34 91 4888088; fax: +34 91 4887068.
E-mail address: alicia.carrero@urjc.es (A. Carrero).

1385-8947/$ – see front matter © 2007 Elsevier B.V. All rights reserved.
doi:10.1016/j.cej.2007.06.022

et al. prepared titanium-substituted SBA-15 catalysts in one step under strong acidic conditions starting from titanocene dichloride with Si/Ti ratios in the range 13–40 [9]; Newalkar et al. synthesized Ti-SBA-15 (Si/Ti = 5–40) [11] and Zr-SBA-15 (Si/Zr = 20–80) [12] mesoporous materials by means of a direct method under micro-wave-hydrothermal conditions; Wei et al. developed a direct synthesis method for in situ coating SBA-15 with MgO by adding magnesium acetate salt into the initial mixture [13]; Wang et al. used a sol–gel method to obtain directly Fe-SBA-15 materials (Si/Fe = 16 and 33) using $Fe(NO_3)_3$ as metal precursor and adjusting the pH to 7 with ammonia [14]; besides, a new approach to the direct synthesis of Cu-SBA-15 materials using H_3PO_4 as acid source and $Al(NO_3)_3$ as concomitant salt has been reported [15]. According to the literature, pH control and type of metal precursor are the main variables to obtain highly ordered mesoporous materials and a high metal incorporation degree [16].

In this paper we report a novel direct synthesis method to prepare CrAlSBA-15 catalysts with different Si/Cr ratios using a non-ionic structure-directing agent. The influence of the chromium precursors (chromium nitrate and chromium acetate) and the pH of synthesis gel on the catalysts properties was evaluated. The obtained catalysts were tested in ethylene polymerization reaction and compared to Cr/SiO_2 and Cr/AlSBA-15 prepared by post-synthesis methods like impregnation and grafting.

2. Experimental

2.1. Synthesis of CrAlSBA-15 catalysts

The chromium–aluminium containing SBA-15 mesoporous solids were prepared as follows: 4 g of triblock copolymer EO_{20}-PO_{70}-EO_{20} (Pluronic 123, Aldrich) were dissolved in 150 ml of aqueous HCl at different pH values (0, 1.5 and 3). At the same time, 8.6 g of tetraethylorthosilicate (TEOS, 98%, Aldrich), 0.276 g of aluminium isopropoxide (AIP, >98%, Aldrich) (Si/Al molar ratio = 30) and the calculated amount of chromium precursor: chromium(III) nitrate (99%, Aldrich) or chromium(III) acetate hydroxide (Aldrich) to get Si/Cr molar ratios equal to 10 and 30 were dissolved into 10 ml of the aforementioned aqueous HCl solution. Both mixtures were stirred for 4 h at room temperature and then, the second one was added over the first one. The final solution was stirred for 20 h at 40 °C and, subsequently, aged at 110 °C for 24 h under static conditions. The solid product was recovered by filtration, dried at room temperature overnight and calcined at 600 °C for 5 h (heating rate = 0.4 °C min^{-1}) under air flow. The samples obtained were called Nit-*x* or Acet-*x* where Nit = chromium nitrate, Acet = chromium acetate and *x* = pH of the synthesis gel.

2.2. Synthesis of grafted and impregnated catalysts

Aluminium-containing SBA-15 mesoporous support (Si/Al = 30) was synthesized according to the process previously reported [8,10]. This material, after drying and calcination at 600 °C, was stirred with a solution of chromium(III) nitrate ($Cr(NO_3)_3$, Aldrich) in ethanol (5 g of Cr per 100 g of solid) for 1 h under reflux. Then, solids were recovered by filtration and intensively washed with ethanol. The same calcined Al-SBA-15 sample was impregnated by a wetness procedure with a fixed amount of $Cr(NO_3)_3$ in ethanol to get 1 wt% chromium loading (0.078 g of $Cr(NO_3)_3$ per gram of support). Finally, catalysts were calcined with air up to 600 °C. These two additional catalysts were called AlSBA-I (impregnated sample) and AlSBA-G (grafted sample). Besides, these mesostructured catalysts have been compared with a conventional Cr/SiO_2 catalyst prepared through impregnation of $Cr(NO_3)_3$ onto commercial silica (EP-10, Crosfield) and calcination with air up to 600 °C.

2.3. Catalysts characterization

Chemical composition of the catalyst samples was measured by ICP-atomic emission spectroscopy on a Varian Vista AX CD system. Previously, the sample was digested by acid treatment with H_2SO_4 and HF. Using the results of ICP analysis, real Si/Al and Si/Cr molar ratios of the catalysts as well as metal incorporation degrees were calculated. Nitrogen adsorption–desorption isotherms at 77 K were obtained with a Micromeritics Tristar 3000 apparatus. The samples were previously out-gassed under vacuum at 250 °C for 4 h. Surface areas were calculated with BET equation whereas pore size distributions were determined by the BJH method applied to the adsorption branch of the isotherms. Mean pore size was obtained from the maximum of BJH pore size distribution. X-ray powder diffraction (XRD) data were acquired on a Philips X'PERT MPD diffractometer using Cu Kα radiation. Low angle XRD patterns ($0.6° < 2\theta < 5°$) were obtained using a step size of 0.02° and a counting time of 5 s. Solid state NMR of ^{27}Al nuclei spectra were obtained on a Varian 400 MHz spectrometer with the following conditions: magic-angle spinning at 6 kHz; $\pi/2$ pulse = 3 μs; repetition delay = 2 s. The NMR of ^{27}Al spectra were referenced to hydrated $AlCl_3$. Transmission electron microscopy measurements were performed on a 200 kV Philips Tecnai 20 electron microscope. Diffuse reflectance UV–vis spectra (DRS) of the calcined CrAlSBA-15 mesoporous catalysts were obtained under ambient conditions on a CARY-1 spectrophotometer equipped with a diffuse reflectance accessory in the wavelength range of 200–900 nm. A halon white reflectance standard was used as a reference material. Hexavalent chromium species in calcined catalysts were analyzed by temperature-programmed reduction (TPR) in a TPD/TPR Micromeritics AutoChem 2090 apparatus using a flow of Ar/H_2 (10% of H_2) with a heating rate of 35 °C min^{-1} from 100 to 600 °C. A TC detector was used to determine the hydrogen consumption. Results obtained from TPD/TPR analysis were used to calculate the accessibility of Cr(VI) species in the calcinated catalysts. Hexavalent chromium centres are reduced by hydrogen leading to trivalent chromium centres. So, according to this reduction reaction the amount of accessible hexavalent chromium can be estimated as: Cr(VI) (mol) = [mol of H_2 consumed during TPR analysis] × 2/3.

2.4. Polymerization tests and polymer characterization

Catalytic tests of ethylene polymerization were carried out in a stirred stainless steel reactor of 2 L capacity using ~100 mg of calcined catalyst. Reaction procedure was the same as in previous works [8]. Polymerization activities (kg PE/g Cr h) were calculated dividing the weight of dry PE produced by the weight of chromium in the catalyst.

DSC analysis of the obtained polymers were recorded from 50 to 180 °C (heating rate = 10 °C min^{-1}) with a Mettler Toledo DSC822 apparatus. High load melt index (HLMI) values were determined at 190 °C with a weight load of 21.6 kg using a Ceast 6542/002 extrusion plastometer. The polyethylene bulk density was determined from the dry weight and the volume of the sample in a volumetric tube by liquid displacement. Polymers mean molecular weight and molecular weight distributions were determined by size-exclusion chromatography at 145 °C on a Waters 150C Plus instrument, using 1,2,4-trichlorobenzene as mobile phase. The column set consisted of one PL-Gel 10 μm Mixed B (300 × 7.5 mm) and another Polymer PL-Gel 10 μm 10E6A (300 × 7.5 mm). The columns were calibrated with 11 polystyrene standards (narrow molar mass distribution in the range: 2960–2,700,000) and with one high polydispersity polyethylene standard (from NIST, Mw = 53,070).

3. Results and discussion

3.1. Synthesis of CrAlSBA-15 catalysts. Effect of chromium precursor and pH

Table 1 shows the composition and the metallic incorporation degrees achieved in the preparation of chromium–aluminium-containing SBA-15 catalysts by a direct synthesis procedure. It can be seen that, using both chromium precursors (nitrate and acetate), the incorporation degree of both metals (Cr and Al) increases with the pH of the synthesis gel. This phenomenon is related to the kind of metallic species present in the synthesis mixture at different pH values. So, under strong acid conditions, metals exist only in the cationic form and the heteroatoms cannot be incorporated into the siliceous structure [16]. An increase of the synthesis solution pH allows the formation of oxo species which makes easy the simultaneous condensation of different metals leading to metal-containing SBA-15 materials [16].

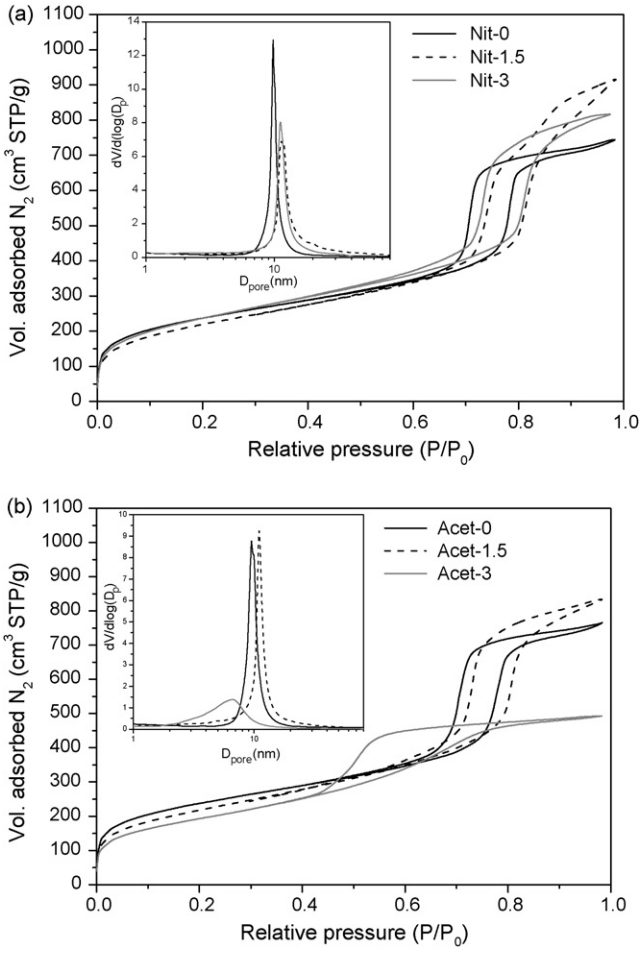

Fig. 1. N_2 adsorption–desorption isotherms at 77 K and pore size distributions of the calcined CrAlSBA-15 catalysts, (a) using chromium nitrate and (b) using chromium acetate.

Fig. 1 displays nitrogen adsorption–desorption isotherms of CrAlSBA-15 catalysts prepared by the direct synthesis method. Samples prepared from chromium nitrate (Fig. 1a) show a clear H1-type hysteresis loop at high relative pressure values, typical for SBA-15 mesoporous materials [10,17]. The slight differences observed at high relative pressures ($P/P_0 > 0.83$) in the hysteresis loop of Nit-1.5 sample indicate that inter-particular adsorption is higher in this material, which can be related with the different shape and size of Nit-1.5 particles. Moreover, the

Table 1
Compositions and metallic incorporation degrees of CrAlSBA-15 catalysts prepared by direct synthesis (Si/Al ratio in the synthesis gel = 30)

Sample	Cr precursor	Synthesis pH	Synthesis Si/Cr ratio	Catalyst Si/Cr ratio[a]	Cr incorpor. degree (%)	Catalyst Si/Al ratio[b]	Al incorpor. degree (%)
Nit-0	$Cr(NO_3)_3$	0	30	615	4.9	263	11.4
Nit-1.5	$Cr(NO_3)_3$	1.5	30	116	25.9	41	73.1
Nit-3	$Cr(NO_3)_3$	3	30	66	60.0	35	85.7
Acet-0	$Cr_3Ac_7OH_2$	0	10	313	3.2	728	4.1
Acet-1.5	$Cr_3Ac_7OH_2$	1.5	10	39	25.6	51	58.9
Acet-3	$Cr_3Ac_7OH_2$	3	10	24	41.7	45	67.7
Acet-3/30	$Cr_3Ac_7OH_2$	3	30	33	90.8	35	85.7

[a] Measured by ICP analysis: $[(Si/Cr)_{synthesis}/(Si/Cr)_{measured}] \times 100$.
[b] Measured by ICP analysis: $[(Si/Al)_{synthesis}/(Si/Al)_{measured}] \times 100$.

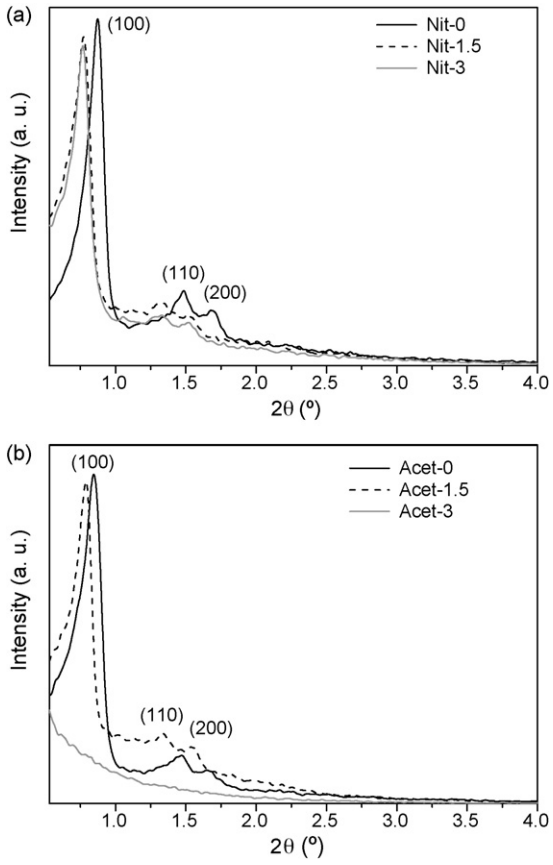

Fig. 2. X-ray diffraction patterns of the calcined CrAlSBA-15 catalysts, (a) using chromium nitrate and (b) using chromium acetate.

pore size distributions of the Nit-0, Nit-1.5 and Nit-3 catalysts are narrow indicating a uniform size of the pores. On the other side, the isotherms and the pore diameters distributions of Acet-0 and Acet-1.5 samples (Fig. 1b) are also characteristic of SBA-15 mesostructured materials, but nitrogen adsorption data of Acet-3 sample indicate a low mesoscopic order. These results were confirmed by X-ray diffraction analysis of calcined samples (Fig. 2). The patterns of the catalysts prepared from chromium nitrate and the samples Acet-0 and Acet-1.5 show well resolved peaks that can be ascribed to the diffraction in the (1 0 0), (1 1 0) and (2 0 0) planes corresponding to the p6mm hexagonal symmetry typical of SBA-15 materials [10,17]. The absence of diffraction signals in the Acet-3 X-ray pattern (Fig. 2b) denotes that this sample has not the usual hexagonal ordering of SBA-15 materials.

Table 2 summarizes the textural and structural properties, determined by nitrogen adsorption–desorption isotherms and by X-ray diffraction analysis, of synthesized CrAlSBA-15 catalysts after the calcination step. It is noticeable that when using chromium nitrate, the growth of pH from 0 to 3 produces an increase of the wall thickness and the $d(1\,0\,0)$ parameter. This tendency could be related to the higher aluminium and chromium content in the catalysts prepared at higher pH values since Al–O and Cr–O bonds are longer than Si–O bond [8,22]. Besides, an increase of pore volume and pore size was detected by increasing the pH value from 0 to 1.5 due to the incorporation of higher amounts of chromium and aluminium. At pH 3, no significant differences in the textural properties were observed since the composition of Nit-1.5 and Nit-3.0 samples are very similar. Only a slight decrease of pore volume is detected by increasing the pH from 1.5 to 3, which is associated with the aforementioned differences between inter-particular adsorption phenomena of Nit-1.5 sample. Using chromium acetate as precursor, similar tendencies were observed increasing the pH value from 0 to 1.5. Acet-3 sample was not compared with Acet-0 and Acet-1.5 mesostructured catalysts due to the before mentioned mesoscopic ordering achieved at pH 3.

Trying to get a CrAlSBA-15 mesostructured material using chromium(III) acetate hydroxide at pH 3, another sample was synthesized with higher Si/Cr ratio (Si/Cr = 30 instead of 10) that is, reducing the amount of basic chromium acetate added to the synthesis mixture. The result was again an amorphous sample called Acet-3/30 which physicochemical properties are also collected in Tables 1 and 2.

To explain the role of chromium precursor on the formation mechanism of mesostructured SBA-15 materials, it has to be taken into account that nitrate anions concentration will remain unaltered during synthesis procedure, while acetate will react with H^+ giving acetic acid according to the equilibrium:

$$CH_3COO^- + H^+ \leftrightarrow CH_3COOH \quad K_a = 1.8 \times 10^{-5};$$

$$pK_a = 4.74$$

since synthesis pH is lower than pK_a the ratio $[CH_3COO^-]/[CH_3COOH] \ggg 1$ and the predominat specie will be acetic acid and no acetate. According to Zhao et al. [17,18], working below pH 2 (isoelectric point of the silica) the formation mechanism of mesostructured SBA-15 materials involves electrostatic interactions between protonated silica

Table 2
Textural and structural properties of CrAlSBA-15 catalysts prepared by direct synthesis

Sample	Si/Cr ratio[a]	Si/Al ratio[a]	A_{BET} (m^2/g)	V_{pore} (cm^3/g)	D_{pore} (nm)	$d(1\,0\,0)$ (nm)	Wall thickness[b] (nm)
Nit-0	615	263	855	1.14	9.8	10.1	1.86
Nit-1.5	116	41	798	1.37	11.3	11.5	1.98
Nit-3	66	35	863	1.27	11.1	11.4	2.06
Acet-0	313	728	855	1.17	9.5	10.4	2.51
Acet-1.5	39	51	790	1.28	10.9	11.2	2.03
Acet-3	24	45	698	0.76	6.8	–	–
Acet-3/30	33	35	880	1.10	8.8	–	–

[a] Determined by ICP analysis.
[b] Wall thickness: a_0—pore size ($a_0 = 2 \times d(100)/\sqrt{3}$).

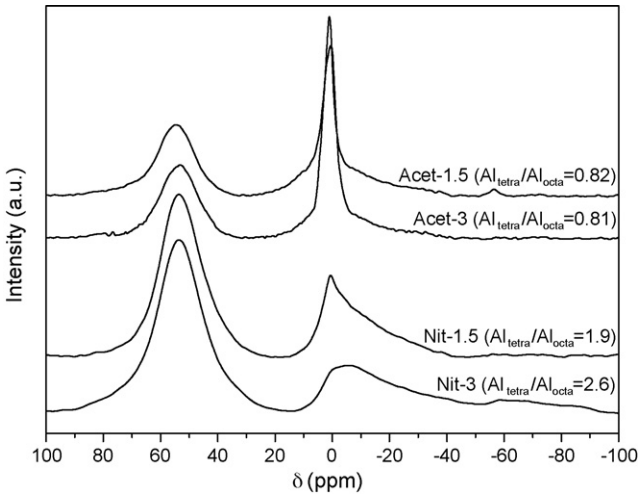

Fig. 3. ^{27}Al NMR spectra of the calcined CrAlSBA-15 catalysts.

(I^+) and protonated surfactant (H^+S^0) by means of inorganic anions (X^-). In this case, acetic acid does not interfere in the mesostructure assembly explaining the high mesoscopic order achieved in Acet-0 and Acet-1.5 samples. However, at pH > 2 silica and surfactant are not protonated and, the assembly of mesostructure occurs by means of hydrogen bonds formation between both neutral phases (S^0I^0) [19]. In this case (pH 3) the acetic acid molecules could establish H-bonds with silica hydroxyl groups or with the surfactant molecules hindering the mesostructure formation and giving amorphous materials like Acet-3 and Acet-3/30. Besides, it is also reported in the literature [20,21] that at lower Si/Cr ratios, like in Acet-3 sample (Si/Cr = 24; 3.2 Cr wt%), a decrease in the ordering of the mesoporous structure is observed.

On the contrary, the interference of nitrate ions on mesostructure assembly must be minimum in both situations: at pH <2 nitrate could have the same behaviour than Cl^- anions, this is,

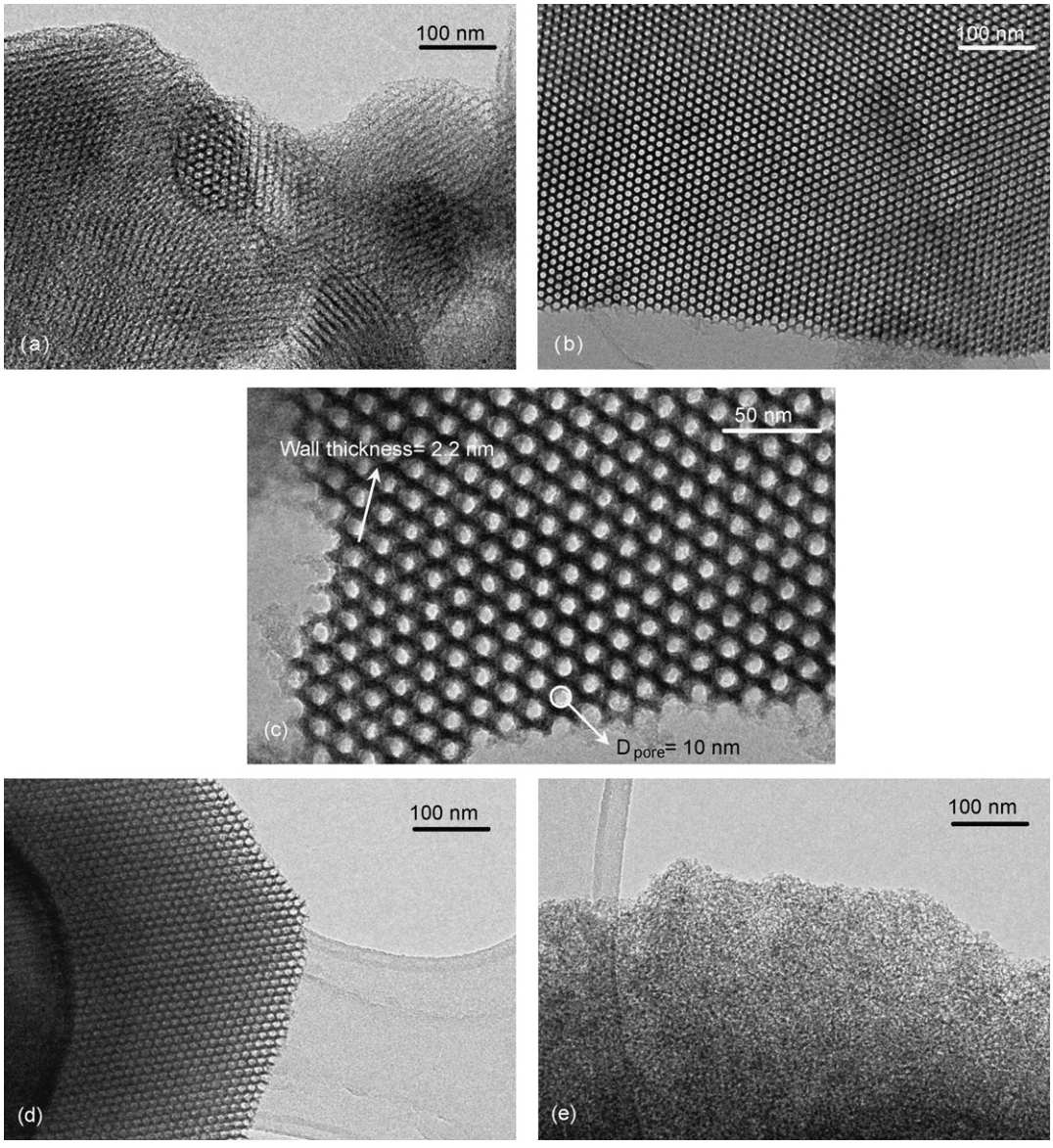

Fig. 4. TEM micrographs of the calcined CrAlSBA-15 catalysts, (a) Nit-1.5, (b) Nit-3, (c) details of Nit-3 structure, (d) Acet-1.5 and (e) Acet-3.

making easier the electrostatic interaction among protonated silica (I^+) and protonated surfactant (H^+N^0); at pH >2, since the formation of mesostructure occurs via H-bonds formation and, the presence of nitrate should not interfere with the assembly process.

The influence of aluminium content on the properties of mesoporous CrAlSBA-15 materials suggests that the incorporation of this heteroatom into the siliceous structure occurs by forming tetrahedral aluminium species which enlarge slightly the unit cell. To confirm the coordination state of aluminium centres, Al^{27} NMR MAS spectra of calcined CrAlSBA-15 materials were carried out. Fig. 3 shows these spectra corresponding to calcined CrAlSBA-15 samples prepared with chromium nitrate and chromium acetate at pH 1.5 and 3 (the spectra of Nit-0 and Acet-0 materials are not shown due to its very low aluminium content). Ratios from tetrahedral to octahedral aluminium species calculated by integration of the corresponding peaks are also showed. The most important signal in Nit-1.5 and Nit-3 spectra is centred at $\delta = 53$ ppm indicating that aluminium atoms are mainly in tetrahedral coordination [23]. However, the lower signal located around 0 ppm, characteristic of octahedral aluminium, suggests that a small quantity of extra-framework aluminium centres (Al_2O_3) are also formed during the synthesis procedure [23]. On the contrary, using chromium acetate as precursor, the main signal appears centred at 0 ppm indicating that octahedral aluminium predominates in Acet-1.5 and Acet-3 samples. High amounts of octahedral aluminium, indicate low condensation degrees of aluminium atoms during the synthesis [24]. This fact may be explained taking into account that Nit-1.5 and Nit-3 samples have a molar ratio Cr/Al = 0.35 and 0.53 respectively, which means that at low chromium contents aluminium atoms can reach tetrahedral positions in the SBA-15 framework. However, Acet-1.5 and Acet-3 have higher chromium contents (Cr/Al = 1.3 and 1.87) and presumably aluminium atoms will compete with chromium for tetrahedral positions.

Transmission electronic microscopy was used to study structural details of calcined CrAlSBA-15 samples. Fig. 4 shows TEM micrographs of Nit-1.5, Nit-3, Acet-1.5 and Acet-3 materials. A perfect hexagonal geometry in the structural ordering can be seen for Nit-1.5 (Fig. 4a), Nit-3 (Fig. 4b) and Acet-1.5 (Fig. 4d) catalysts. These results are in agreement with those previously obtained using X-ray diffraction and nitrogen adsorption–desorption isotherms. Besides, Fig. 4c displays a magnification of Nit-3 pore system in order to compare wall thickness and pore diameter values obtained by TEM and by XRD and N_2 adsorption isotherms; the conclusion is that similar results were achieved. Finally, as expected, TEM micrograph of Acet-3 catalyst (Fig. 4e) shows a disordered porous structure corresponding to an amorphous material.

CrAlSBA-15 materials were characterized by UV–vis spectroscopy to identify the coordination state of chromium atoms in calcined samples. Fig. 5a–d show the UV–vis spectra of calcined Nit-1.5, Nit-3, Acet-1.5 and Acet-3 materials, respectively. All the spectra present three bands located around 240–260 nm, 350–370 nm and 440–460 nm which can be assigned to the $O \rightarrow Cr^{6+}$ charge transfer transitions of chromate and dichromate [25,26]. Specifically, the signal centred at higher wave length (~450 nm) is related to the presence of dichromate

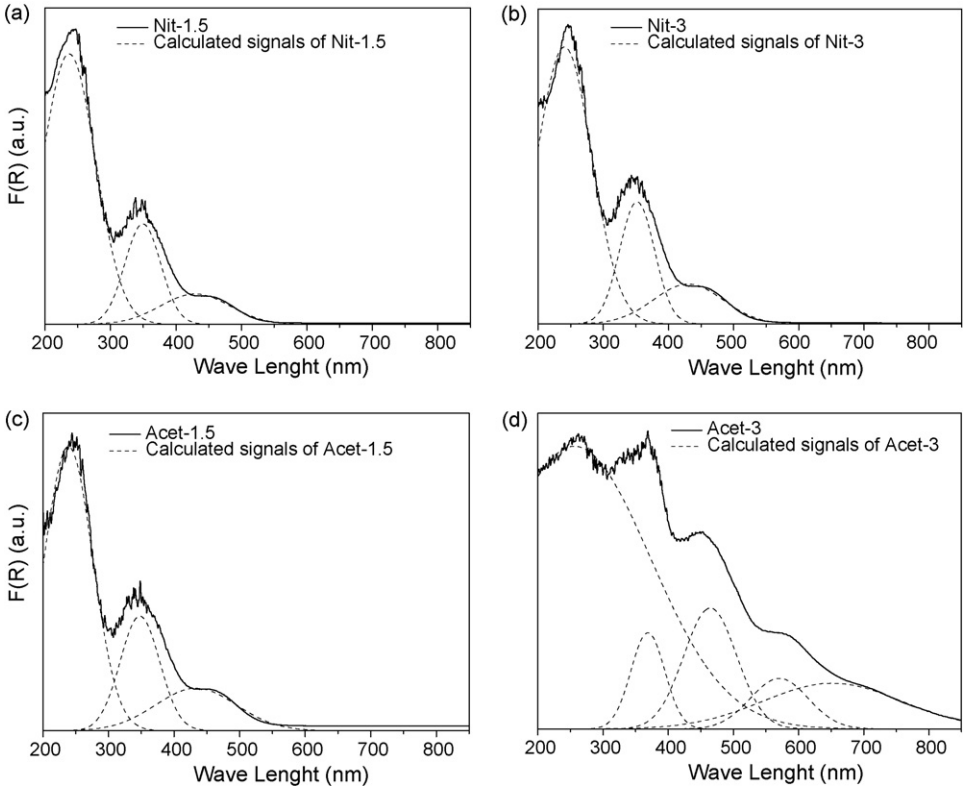

Fig. 5. UV–vis spectra of calcined CrAlSBA-15 catalysts, (a) Nit-1.5, (b) Nit-3, (c) Acet-1.5 and (d) Acet-3.

species, the signal located around 360 nm is due to chromate species whereas the peak centred at lower wave length (~250 nm) can be associated to the presence of both chromate and dichromate [25,26]. In the spectrum of Acet-3 sample, two additional bands located at 570 and 660 nm are observed; these signals are attributed to electronic transitions of pseudo-octahedral coordinated chromium(III) ions [25] and, therefore, indicate the presence of Cr_2O_3 species in the structure of calcined Acet-3 sample. This chromium species distribution on the support surface is close to the distribution achieved by chromium incorporation using post-synthesis procedures like grafting or conventional impregnation [7,8].

The presence of Cr(III) bands detected only in the spectrum of Acet-3 catalyst may be related to the higher chromium content of this sample (Si/Cr = 24; Cr = 3.2 wt%). Previous works have reported that Cr_2O_3-formation is the most pronounced on Cr/SiO_2 catalysts with high Cr loadings [1,27,28]. Thus, as the chromium loading increases, almost all Cr is stabilized in the hexavalent state until certain saturation coverage is reached. Beyond this limit, excess Cr is converted to Cr_2O_3 [1].

3.2. Comparison among the different chromium incorporation methods

Considering the properties of all CrAlSBA-15 catalysts prepared by direct synthesis and previously characterized, Nit-1.5 sample was chosen to be tested in ethylene polymerization since its pore volume is the highest and its chromium content is suitable to be used in slurry phase polymerization processes. Besides, two additional samples were prepared and tested in ethylene polymerization reaction in order to evaluate the influence the of catalyst preparation method. In one case, the chromium was incorporated by impregnation (AlSBA-I sample) and, in the other one by grafting (AlSBA-G) using chromium nitrate as precursor [7,8]. Table 3 summarizes the textural properties and the chromium contents of the three mesostructured chromium catalysts tested in ethylene polymerization. As it can be seen, both textural properties and chromium contents are very similar in all cases.

After activation, the three catalysts were characterized by H_2 temperature programmed reduction (TPR) and UV–vis spectroscopy in order to know the influence of preparation method on the formation and reduction of Cr(VI) active sites. Fig. 6 shows H_2-TPR profiles of activated catalysts along with the individual peaks obtained using computer deconvolution. The three samples present a single signal that suggests a single reduction step from hexavalent to trivalent chromium species due to the reaction with H_2 [29–33]. However, after deconvolution it can be seen that AlSBA-I and Nit-1.5 catalysts show only one kind of Cr(VI) species whereas the signal of AlSBA-G is the result of two peaks indicating the presence of two Cr(VI) species. The peak located at higher temperature (375 °C) is usually assigned to chromate and dichromate reduction while the low temperature TPR peak (330 °C) can be related to the reduction of agglomerated Cr(VI) oxide species which appear after the hydrolysis of Si–O–Cr and Al–O–Cr bonds [31]. In this way and considering the TPR signals observed in these samples, Cr(VI) oxide would be the predominant chromium species in AlSBA-I cat-

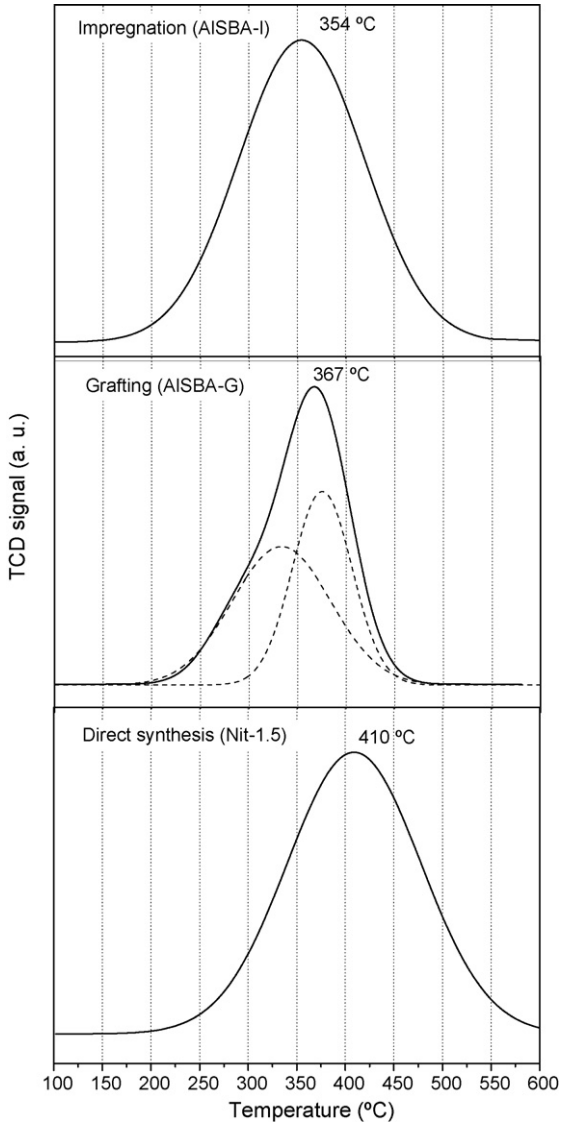

Fig. 6. H_2-TPR profiles of activated chromium-containing AlSBA-15 catalysts.

Table 3
Textural and structural properties of AlSBA-15 chromium catalysts tested in ethylene polymerization.

Catalysts	Si/Al ratio	$[Al_{tetra}/Al_{octa}]^a$	Cr content (wt%)	A_{BET} (m^2/g)	V_{pore} (cm^3/g)	D_{pore} (nm)	$d(1\,0\,0)$ (nm)	Wall thickness (nm)
AlSBA-I	38	2.0	0.91	675	1.20	11.7	11.3	1.35
AlSBA-G	38	2.0	0.77	690	1.23	11.8	11.3	1.25
Nit-1.5	41	1.9	0.72	798	1.37	11.3	11.5	1.98

[a] Determined from ^{27}Al-NMR spectra (area $\delta = 53$ ppm/area $\delta = 0$ ppm).

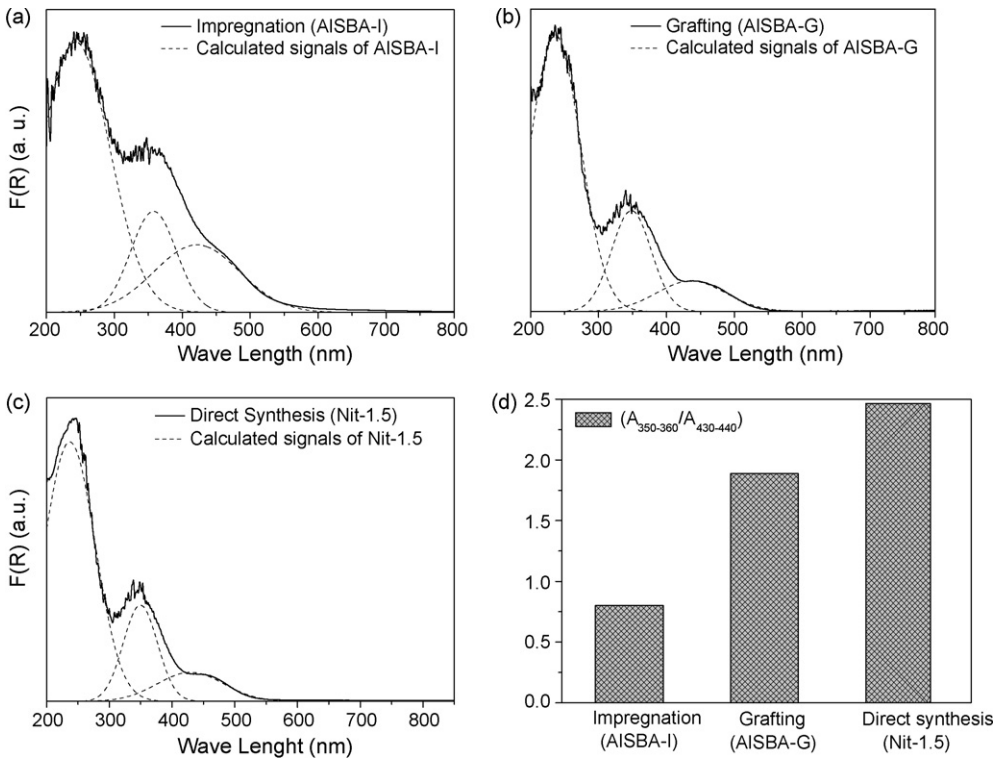

Fig. 7. UV–vis spectra of activated chromium-containing AlSBA-15 catalysts, (a) AlSBA-I, (b) AlSBA-G, (c) Nit-1.5 and (d) chromate to dichromate ratio of chromium-containing AlSBA-15 catalysts calculated from the deconvoluted spectra of calcined samples.

alyst and chromate–dichromate in the Nit-1.5 material. These observations are directly related to the chromium incorporation method since impregnation will result in lower metallic dispersion making easier the agglomeration of Cr(VI) centres and, thus producing chromium species which can be reduced by hydrogen at lower temperatures. On the contrary, the direct synthesis procedure will provide better dispersed metallic centres and, therefore, higher amounts of chromate-dichromate can be obtained. Finally, the grafting method allows to get a mixture of both Cr(VI) oxide and chromate–dichromate species.

The ratio between chromate and dichromate species can be estimated by means of UV–vis spectra of activated catalysts. Thus, Fig. 7(a–c) show the UV–vis spectra of calcined AlSBA-I, AlSBA-G and Nit-1.5 catalysts, respectively, and their corresponding deconvolutioned peaks. It can be observed that all catalysts present three signals centred around 230–240 nm, 350–360 nm and 430–440 nm which are assigned to the $O \rightarrow Cr^{6+}$ charge transfer transitions of chromate and dichromate [25,26]. Considering the area values of the signals located around 350 nm (chromate) and 430 nm (dichromate) a ratio between both kind of Cr(VI) centres can be estimated. The result of this estimation is presented in Fig. 7(d). It is remarkable that a very important growth of chromate signal is observed changing the catalyst preparation method from impregnation to direct synthesis.

3.3. Polymerization tests

Finally, ethylene polymerization reactions were carried out in order to know the relation between the preparation method and the catalytic behaviour. Table 4 presents the ethylene polymerization activities of AlSBA-I, AlSBA-G, Nit-1.5 and a conventional Phillips Cr/SiO_2 catalyst, as well as the main properties of the resulting polymers: molecular weight, melt temperature, high load melt index (HLMI) and bulk density.

As observed, better polymerization activities are observed when using samples prepared by grafting or direct synthesis methods as compared to those prepared by impregnation. Focus-

Table 4
Ethylene polymerization results obtained with AlSBA-15 chromium catalysts (polymerization conditions: $T = 90\,^{\circ}C$; $P_{ethylene} = 35$ bar; $P_{hydrogen} = 5.0$ bar; 0.5 mol of 1-hexene; solvent = isobutane)

Catalyst	Activity (kg PE/g Cr h)	Mw	T_m (°C)[a]	HLMI (g/10 min)	Bulk density (g/ml)
AlSBA-I	260.5	433970	130.5	3.9	0.24
AlSBA-G	460.1	428430	131.4	5.0	0.29
Nit-1.5	381.1	395480	131.5	2.8	0.24
Cr/SiO_2[b]	216.0	531100	132.5	2.3	0.30

[a] Melting temperature measured by DSC.
[b] Conventional Phillips catalyst prepared by silica impregnation.

Table 5
Accessibility of chromium centres estimated by H_2 TPR analysis and polymerization activities calculated per accessible chromium centre

Catalysts	Cr content (wt %)	H_2 consumed (mmol/g)	Accessibility of Cr centres (%)[a]	Activity (kg PE/g $Cr_{accessible}$ h)
AlSBA-I	0.91	0.240	91.3	285.3
AlSBA-G	0.77	0.206	92.9	495.3
Nit-1.5	0.72	0.155	80.7	472.2

[a] Calculated by $((2/3)A/B) \times 100$ where A: mol of H_2 consumed during TPR analysis and B: mol of Cr determined by ICP in the catalyst.

ing on grafting and direct synthesis samples, the higher activity of AlSBA-G catalyst could be explained by the lower accessibility of chromium centres in the sample prepared by direct synthesis. The metal incorporation into mesoporous SBA-15 structure using one-step synthesis procedure involves that a fraction of the metallic centres can remain in non-accessible positions inside of the solid walls. In this case, both impregnation and grafting procedures would lead to superficial easier accessible chromium centres but, for the catalyst prepared by direct synthesis, non-accessible chromium centres could be formed. This fact was confirmed from the data obtained by integration of H_2 TPR signals. Table 5 shows the percentages of accessible chromium centres in the AlSBA-I, AlSBA-G and Nit-1.5 catalysts and the corresponding activity values now calculated taking into account this accessibility factor. So, it can be seen that the activity of the grafted catalyst and the one-step synthesis catalyst are very similar and around a seventy percent higher that the activity for the impregnated catalyst. Theses results can be explained considering the better dispersion of the metallic centres (and therefore the higher proportion of chromate species) existing in AlSBA-G and Nit-1.5 samples in comparison with the impregnated one. Therefore, one important conclusion of this work is that a novel Phillips catalyst much more active than the conventional ones can be obtained by a one-step synthesis procedure.

Concerning the obtained polymers, it is remarkable that mesostructured catalysts produced high density polyethylene with very similar properties: melting temperatures around 131 °C, molecular weights (MW) in the range of 4×10^5 and bulk densities between 0.24 and 0.29 g/cm^3. Only high load melt index values show slight variations depending on the catalyst used which could be related to the different proportion of long chain branching in polyethylene structure produced by each catalyst [34].

4. Conclusions

A new one-step direct synthesis method to prepare CrAlSBA-15 materials was developed using different chromium precursors (chromium(III) nitrate and acetate hydroxide) and pH values (0, 1.5 and 3). A very important increase of Cr and Al incorporation degrees was achieved increasing the pH from 0 to 3.

Chromium nitrate led to CrAlSBA-15 materials with high mesostructural order with a Si/Cr of 66 and Si/Al of 35. However, an amorphous material was obtained using chromium acetate hydroxide at pH 3. In this case, CH_3COOH formed by protonation of acetate anions can establish H-bonds with the silica and/or surfactant molecules hindering the mesostructure formation.

The incorporation of chromium and aluminium into SBA-15 mesoporous structure produces an increase in pore size and pore volume. After calcination, samples prepared by one-step synthesis showed Cr(VI) centres well dispersed with a proportion of chromate species higher than Cr/AlSBA-15 catalysts prepared by post-synthesis methods like impregnation and grafting. H_2-TPR measurements showed that only the 80% of Cr(VI) ions incorporated into the SBA-15 structure are reduced, so part of chromium ions may be located in non-accessible positions inside the solid walls.

CrAlSBA-15 materials obtained by direct synthesis exhibited higher polymerization activity (381.1 kg PE/g Cr h) than Cr/AlSBA-15 and conventional Cr/SiO_2 Phillips catalyst prepared by impregnation (260.5 and 216 kg PE/g Cr h, respectively). According to these results, it is concluded that novel active chromium catalysts can be obtained by the one-step synthesis route showed in this paper, performing better than conventional Phillips polymerization catalysts.

References

[1] B.M. Weckhuysen, R.A. Schoonheydt, Catal. Today. 51 (1999) 215.
[2] E. Groppo, C. Lamberti, S. Bordiga, G. Spoto, A. Zecchina, Chem. Rev. 105 (2005) 115.
[3] E. Groppo, C. Lamberti, S. Bordiga, G. Spoto, A. Zecchina, J. Catal. 240 (2006) 172.
[4] B.M. Weckhuysen, R.A. Schoonheydt, Chem. Comm. (1999) 445.
[5] B.M. Weckhuysen, R. Ramachandra, J. Pelgrims, R.A. Schoonheydt, P. Bodart, G. Debras, O. Collart, P. Van Der Voort, E.F. Vansant, Chem. Eur. J. 6 (2000) 2960.
[6] G. Calleja, J. Aguado, A. Carrero, J. Moreno, Catal. Commun. 6 (2005) 153.
[7] G. Calleja, J. Aguado, A. Carrero, J. Moreno, Stud. Surf. Sci. Catal. 158 B (2005) 1453.
[8] G. Calleja, J. Aguado, A. Carrero, J. Moreno, App. Catal. A Gen. 316 (2007) 22.
[9] J.A. Melero, J.M. Arsuaga, P. de Frutos, J. Iglesias, J. Sainz, S. Blázquez, Microporous Mesoporous Mater. 1–3 (2005) 364.
[10] Y. Yue, A. Gédéon, J.-L. Bonardet, N. Melosh, J.-B. D'Espinose, J. Fraissard, Chem. Commun. (1999) 1967.
[11] B.L. Newalkar, J. Olanrewaju, S. Komarneni, Chem. Mater. 13 (2001) 552.
[12] B.L. Newalkar, J. Olanrewaju, S. Komarneni, J. Phys. Chem. B 105 (2001) 8356.
[13] Y.L. Wei, Y.M. Wang, J.H. Zhu, Z.Y. Wu, Adv. Mater. 15 (2003) 1943.
[14] X.Q. Wang, H.L. Ge, H.X. Jin, Y.J. Cui, Microporous Mesoporous Mater. 1–3 (2005) 335.
[15] L. Wang, A. Kong, B. Chen, H. Ding, Y. Shan, M. He, J. Mol. Catal. A: Chem. 1–2 (2004) 143.
[16] S. Wu, Y. Han, Y.-C. Zou, J.-W. Song, L. Zhao, Y. Din, S.-Z. Liu, F.-S. Xiao, Chem. Mater. 16 (2004) 486.
[17] D. Zhao, J. Feng, Q. Huo, N. Melosh, G.H. Fredrickson, B.F. Chmelka, G.D. Stucky, Science 279 (1998) 548.
[18] D. Zhao, Q. Huo, J. Feng, B.F. Chmelka, G.D. Stucky, J. Am. Chem. Soc. 120 (1998) 6024.

[19] G.J.A.A. Soler-Illia, E.L. Crepaldi, D. Grosso, C. Sánchez, Curr. Opin. Colloid Interface Sci. 8 (2003) 109.
[20] S. Rodrigues, K.T. Ranjit, S. Uma, I.N. Martyanov, K.J. Klabunde, J. Catal. 230 (2005) 158.
[21] X. Zhao, X. Wang, J. Mol. Catal. A: Chem. 261 (2007) 225.
[22] M. Selvaraj, S. Kawi, Chem. Mater. 19 (2007) 509.
[23] A. Matsumoto, H. Chen, K. Tsutsumi, M. Grün, K. Unger, Microporous Mesoporous Mater. 32 (1999) 55.
[24] W. Hu, Q. Luo, Y. Su, L. Chen, Y. Yue, C. Ye, F. Deng, Microporous Mesoporous Mater. 92 (2006) 22.
[25] B.M. Weckhuysen, I.E. Wachs, R.A. Schoonheydt, Chem. Rev. 96 (1996) 3327.
[26] B.M. Weckhuysen, L.M. De Ridder, R.A. Schoonheydt, J. Phys. Chem. 97 (1993) 4756.
[27] M.P. McDaniel, J. Catal. 76 (1982) 37.
[28] M.P. McDaniel, Adv. Catal. 33 (1985) 47.
[29] A. Ellison, T.L. Overton, L. Bencze, J. Chem. Soc. Faraday Trans. 89 (1993) 843.
[30] A.B. Gaspar, J.L.F. Brito, L.C. Dieguez, J. Mol. Catal. A: Chem. 203 (2003) 251.
[31] C.S. Kim, S.I. Woo, J. Mol. Catal. 73 (1992) 249.
[32] J. Santamaría-González, J. Mérida-Robles, M. Alcántara-Rodríguez, P. Maireles-Torres, E. Rodríguez-Castellón, A. Jiménez-López, Catal. Lett. 64 (2000) 209.
[33] M. Cherian, M.S. Rao, A.M. Hirt, I.E. Wachs, G. Deo, J. Catal. 211 (2002) 482.
[34] M.P. McDaniel, D.C. Rohlfing, E.A. Benham, Polym. React. Eng. 11 (2003) 101.